1

From Dendrites to Labyrinths: The Morphology of Magnetic Flux Patterns in Superconductors[1]

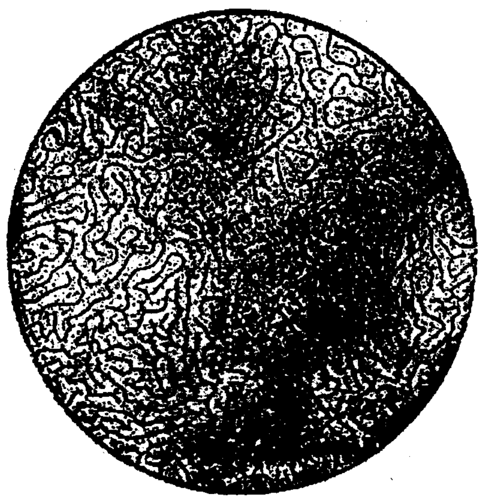

A. T. Dorsey, *Department of Physics, University of Florida*

Collaborators: R. Goldstein (*U. Arizona*), A. Dolgert, S.J. Di Bartolo (*U. Virginia*).

[redacted]

2

Type-I Superconductivity

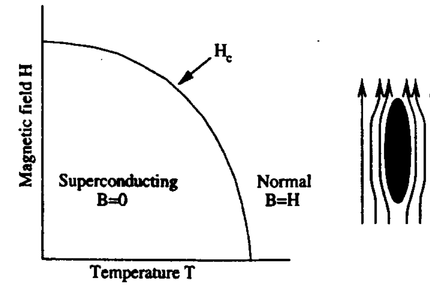

- What happens in a thin film?

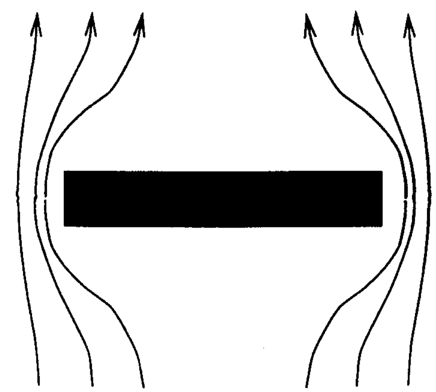

- Such a configuration is energetically unfavorable. The sample breaks up into normal and superconducting regions→intermediate state.

Dorsey
Lecture 4

From R. P. Huebener, "Magnetic Flux Structures in Superconductors"

Field out of page ⊙$\vec{H}$

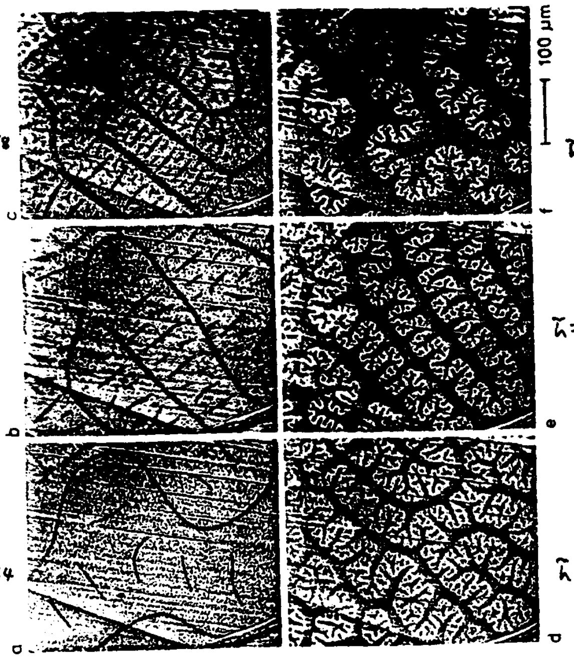

Fig.2.17a-f. Intermediate state of the same Pb disk as in Fig.2.9 in perpendicular magnetic field for decreasing values of $\tilde{h} = H/H_c$. (a) $\tilde{h} = 0.84$, (b) $\tilde{h} = 0.74$, (c) $\tilde{h} = 0.58$, (d) $\tilde{h} = 0.42$, (e) $\tilde{h} = 0.32$, (f) $\tilde{h} = 0.21$. Normal phase is bright, T = 4.2 K, $(NI)_T$ transition. (Courtesy of A. Kiendl)

Magnetic field pattern in a type-I superconductor — "intermediate state"

Path Dependence of Structures

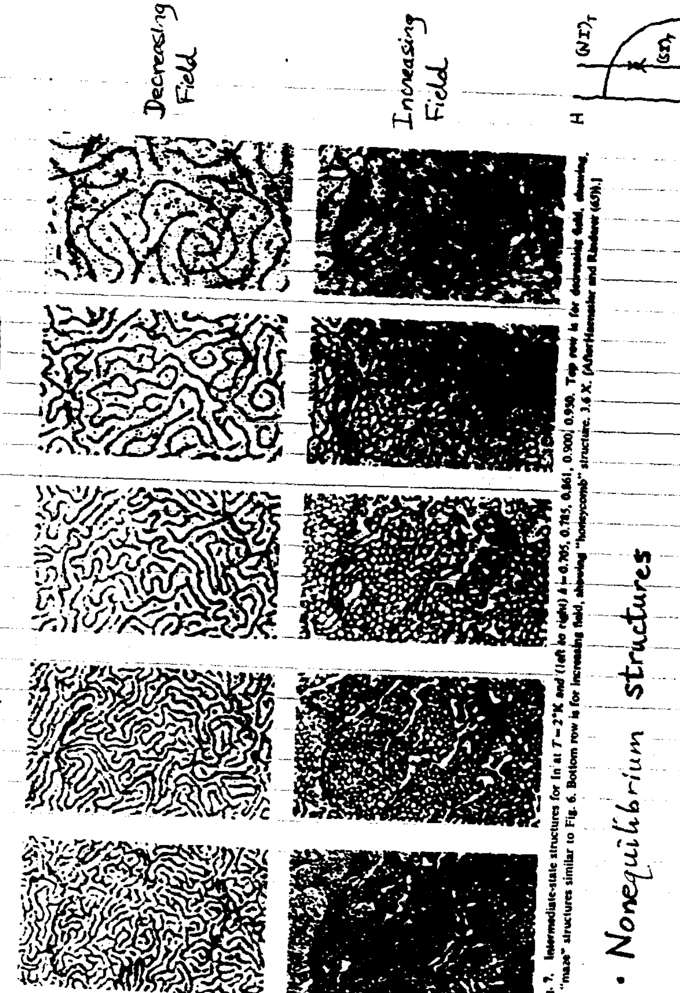

Fig. 7. Intermediate-state structures for In at $T \sim 2°K$ and (left to right) $h = 0.705, 0.785, 0.861, 0.900, 0.950$. Top row is for decreasing field, showing "maze" structures similar to Fig. 6. Bottom row is for increasing field, showing "honeycomb" structure. 3.6 X. [After Haenssler and Rinderer (459).]

• Nonequilibrium structures

5

Issues:

- Many of the patterns involve sharp interfaces between two phases: either normal/superconducting, superconducting/vortex liquid, etc. Focus on developing models for the interface dynamics.
- Can we understand
  - length scales?
  - topology?
  - dynamics?

Outline:

- Interface dynamics without demagnetizing effects.
  - Growth of the superconducting phase—a free boundary model.
  - Instabilities of the interface motion and analogies with dendritic growth.
  - Studies using the time-dependent Ginzburg-Landau equations.
  - Experiments.
- Including demagnetizing effects—the intermediate state.
  - Landau's model of the intermediate state.
  - The current loop model of the intermediate state.
  - Numerical studies of branching instabilities.
  - The laminar state—energetics, fluctuations, and defects.
  - Experiments.

6

From R. P. Feynman, ***The Feynman Lectures on Physics, Vol. II:***

> Finally, there is a most remarkable coincidence: *The equations for many different physical situations have exactly the same appearance.* Of course, the symbols may be different—one letter is substituted for another—but the mathematical form of the equations is the same. This means that having studied one subject, we have a great deal of direct and precise knowledge about the solutions of the equations of another.

7

Interface Dynamics in Superconductors

How is the magnetic flux expelled from the Meissner phase? Consider a type-I superconductor (*without demagnetizing effects*).

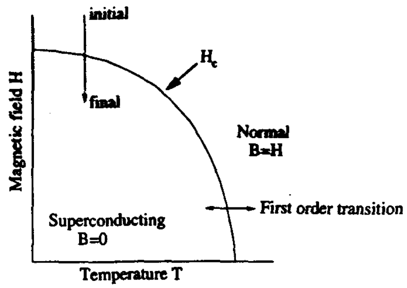

$H_{external} < H_c$

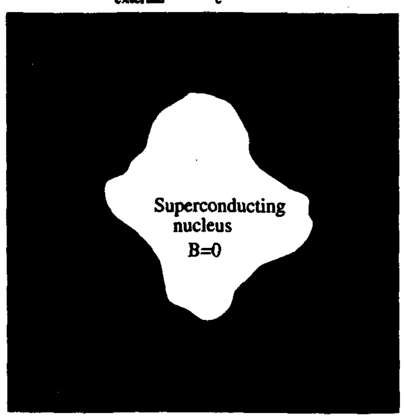

8

Free boundary model for interface motion

- In the normal phase eddy currents are produced due to flux motion. Faraday's law + Ampère's law + Ohm's law ($\mathbf{J} = \sigma \mathbf{E}$) leads to the diffusion equation for the B field ($\mathbf{B} = B(x,y)\hat{z}$), with $D_B = c^2/4\pi\sigma$:

$$\partial_t B = D_B \nabla^2 B \quad \text{(normal regions)}.$$

- In the superconducting regions $B = 0$.
- On the normal side of the S/N interface, $\mathbf{E} = -\mathbf{v} \times \mathbf{B}$, so that $E_t = v_n B_i$ (t = tangent, n = normal). Combine with Ohm's law and Ampere's law to arrive at the boundary condition on the moving boundary:

$$B_i v_n = -D_B (\partial B/\partial n)|_i.$$

- For an equilibrium, planar S/N interface, $B = H_c$ as the interface is approached from the superconducting side. If the interface has curvature $\mathcal{K}$, and moving with a normal velocity v_n, this becomes

$$B_i = H_c(1 - d_0\mathcal{K} - \beta v_n),$$

where d_0 is the capillary length and β is the kinetic coefficient.

- Far from the S/N interface the magnetic field is the applied field.
- The diffusion equations + boundary conditions constitute a free boundary problem for the moving interface. It is highly nonlinear and nonlocal; analytic solutions are only known for zero surface tension and in special circumstances.

Dendritic growth of a pure substance

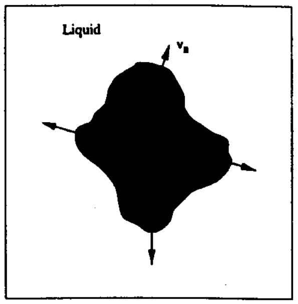

$T_{wall} < T_{melt}$

- Place a piece of a solid into its supercooled liquid. The conversion of liquid into solid produces latent heat L, which must diffuse away from the interface in order for the solid to continue growing:

$$\partial_t T = D_T \nabla^2 T.$$

- At the interface,

$$\underbrace{L v_n}_{\text{rate of heat production}} = \underbrace{\left[D'_T c'_P (\partial T/\partial n)_{\text{solid}} - D_T c_P (\partial T/\partial n)_{\text{liquid}}\right]}_{\text{rate at which heat flows into liquid and solid}}.$$

- The temperature at the planar solid/liquid interface is the melting temperature T_m; for a curved, moving interface we have the Gibbs-Thomson boundary condition:

$$T_i = T_m(1 - d_0\mathcal{K} - \beta v_n),$$

with d_0 the capillary length, $\mathcal{K}$ the curvature, and β a kinetic coefficient.

Dendritic growth $\Longleftrightarrow$ flux expulsion[2]

- There is a close analogy between **flux** expulsion and dendritic growth:

Flux expulsion	Solidification
Flux diffuses away from the interface.	Heat diffuses away from the interface.
Flux diffusion: $\partial_t B = D_B \nabla^2 B$	Thermal diffusion: $\partial_t T = D_T \nabla^2 T$
$D_B = c^2/4\pi\sigma \sim 10$ cm^2 s^{-1}	$D_T \sim 10^{-3}$ cm^2 s^{-1}
Faraday's law: $B_i v_n = -D_B(\partial B/\partial n)\|_i$	Heat flux: $L v_n = -D_T c_P (\partial T/\partial n)\|_i$
$B_i = H_c(1 - d_0\mathcal{K} - \beta v_n)$	Gibbs-Thomson: $T_i = T_m(1 - d_0\mathcal{K} - \beta v_n)$
Instability: "fingered" flux fronts.	Instability: Mullins-Sekerka (dendrites).

- There should be a dynamic instability of the flux front, which is only stabilized at short wavelengths due to surface tension effects.

[2]Frahm, Ullah, and Dorsey, Phys. Rev. Lett. **66**, 3067 (1991); Liu, Mondello, and Goldenfeld, Phys. Rev. Lett. **66**, 3071 (1991)

(11)

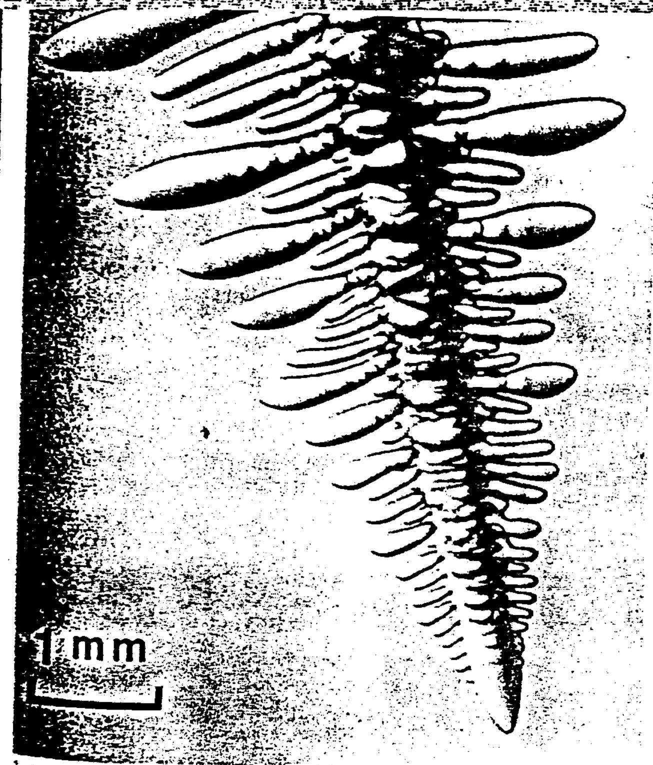

Fig. 1. Primary dendrite of succinonitrile (a transparent plastic crystal with cubic symmetry) growing in its undercooled melt. Note the smooth paraboloidal tip, the secondary sidebranching oscillations emerging behind the tip, and the beginnings of tertiary structure on the well-developed secondaries. (Photograph courtesy of M. E. Glicksman.)

8a

(12)

Dynamic instabilities of the interface

- In the solidification problem, the growth is known to be unstable; highly ramified patterns are formed ("dendrites"). Therefore we expect the growing superconducting nucleus to also be dynamically unstable!

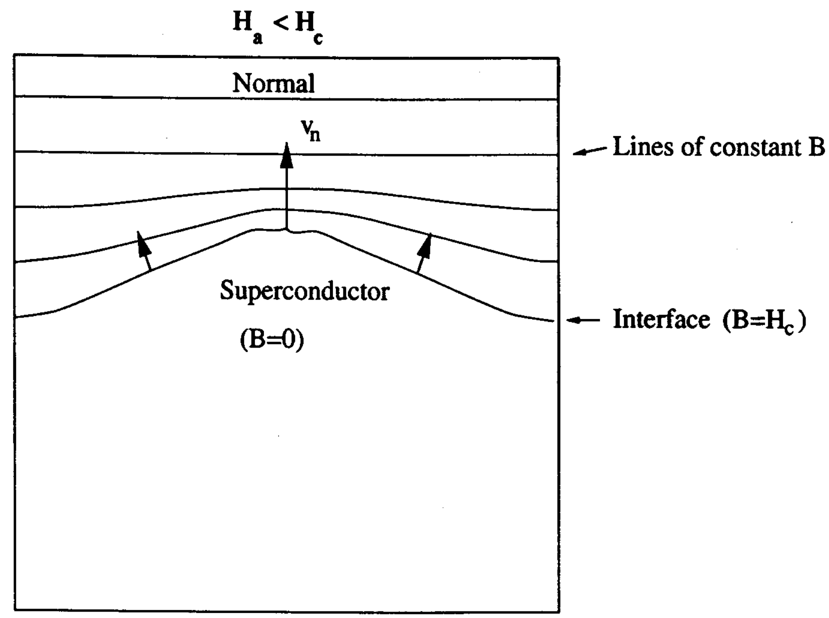

- $\partial B/\partial n$ is largest near the bump; recalling that $B_i v_n = -D_B(\partial B/\partial n)|_i$, we see that *bumps grow faster.*

(13)

- A linear stability analysis for a planar interface shows that the growth rate for long wavelength perturbations is positive, and is stabilized at short wavelengths by the surface tension:

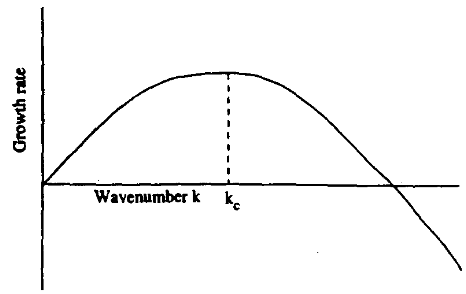

- In the solidification problem, the crystalline anisotropy will "focus" the instability, leading to dendritic patterns ("snowflakes").

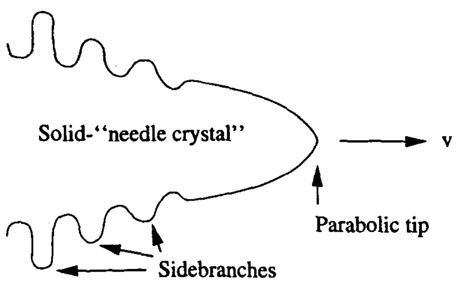

(14)

A demonstration[3]

- A model for "Poisson growth": see H. La Roche *et al.*, Phys. Rev. A **44**, R6185 (1991).
- Two glass plates separated by grease.
- Slowly lift the top plate.

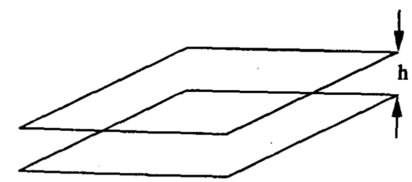

- Mass conservation gives

$$\partial_t h = -h\nabla \cdot \mathbf{v}.$$

- Combine with *Darcy's law*,

$$\mathbf{v} = -k\mu\nabla p$$

(for Poiseuille flow $k = h^2/12$); assuming gradients in h are small,

$$\nabla^2 p = \frac{\mu}{k}\left[\frac{1}{h}\frac{\partial h}{\partial t}\right].$$

- At the interface, $v_n \propto -\partial p/\partial n$.

[3]Special thanks to Chris Lobb.

15

Time-dependent Ginzburg-Landau (TDGL) theory

- The TDGL equations for the order parameter ψ and the vector potential $\mathbf{A}$ are

$$\begin{aligned} \hbar\gamma\left(\partial_t + \frac{ie^*}{\hbar}\phi\right)\psi &= -\frac{\delta\mathcal{F}}{\delta\psi^*} = \frac{\hbar^2}{2m}\left(\nabla - \frac{ie^*}{\hbar}\mathbf{A}\right)^2\psi + a\psi - b|\psi|^2\psi, \\ \nabla\times\nabla\times\mathbf{A} &= 4\pi\left(\mathbf{J}_n + \mathbf{J}_s\right)\ , \end{aligned}$$

where $\mathbf{J}_n$ and $\mathbf{J}_s$ are the normal and supercurrents,

$$\begin{aligned} \mathbf{J}_n &= \sigma\left(-\nabla\phi - \partial_t\mathbf{A}\right) \\ \mathbf{J}_s &= \frac{\hbar e^*}{2mi}\left(\psi^*\nabla\psi - \psi\nabla\psi^*\right) - \frac{e^{*2}}{m}|\psi|^2\mathbf{A}\ . \end{aligned}$$

The parameter $a = a_0\left(1 - T/T_c\right)$ and controls the correlation length $\xi = \hbar/(2m|a|)^{1/2}$ and penetration depth $\lambda = \left[mb/4\pi e^{*2}|a|\right]^{1/2}$. The magnetic field is $\mathbf{H} = \nabla\times\mathbf{A}$.

- Important dimensionless parameters: $\kappa = \lambda/\xi$ (ratio of length scales), $\bar{\sigma} = 4\pi\kappa^2(\hbar\sigma/2m\gamma)$ (ratio of time scales).
- Can be derived from the microscopic BCS theory in the appropriate limit.
- Can derive interface model from TDGL equations using matched asymptotic expansions.[4] The constants d_0, β are determined from solutions of the equilibrium GL equations.[5]

[4] A. T. Dorsey, Ann. Phys. **233**, 248 (1994); S. J. Chapman, Quart. Appl. Math. **53**, 601 (1995).

[5] J. C. Osborn and A. T. Dorsey, Phys. Rev. B **50**, 15 961–15 966 (1994).

16

Numerical solution of the TDGL equations

- Computational lattice:

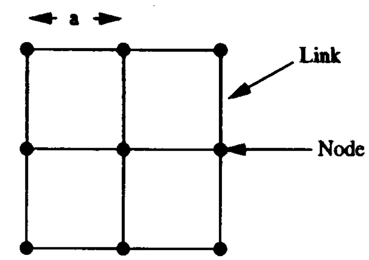

- Discretize TDGL equations. Put gauge fields on the links of the lattice to insure gauge invariance ($\mu = x, y$):

$$U^\mu(\mathbf{x}) = \exp[-i\kappa a A_\mu(\mathbf{x})].$$

Then derivatives become

$$\left(\frac{1}{2i\kappa}\partial_\mu - iA_\mu\right)\psi \to \frac{1}{i\kappa a}\left[U^\mu(\mathbf{x})\psi(\mathbf{x} + a\hat{\mu}) - \psi(\mathbf{x})\right],$$

$$(\nabla\times\mathbf{A})_z \to -\frac{1}{i\kappa a^2}\left\{U^x(\mathbf{x})U^y(\mathbf{x} + a\hat{x})\left[U^x(\mathbf{x} + a\hat{y})\right]^{-1}\left[U^y(\mathbf{x})\right]^{-1} - 1\right\}.$$

Becomes a *lattice gauge theory.*

- Iterate equations of motion.

H. Frahm, S. Ullah, A.T. Dorsey, PRL 66, 3067 (1991)

Numerical Solution of TDGL Equations

Time →

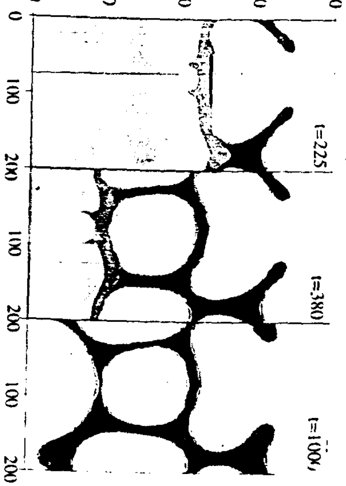

FIG. 2. The magnetic field for a type-I superconductor in the *spinodal* regime. The initial conditions and relevant parameters are the same as in Fig. 1 except that $H_c = 0.2$. There is no lower critical size for seed nucleation so that the order parameter can leak through the flux wall via the mechanism of phase slippage (see text), resulting in a daughter seed on the other side of the wall. The daughter seed continues to grow until once more the field at the interface increases to H_c, and the process repeats.

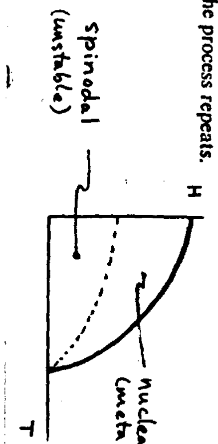

Time →

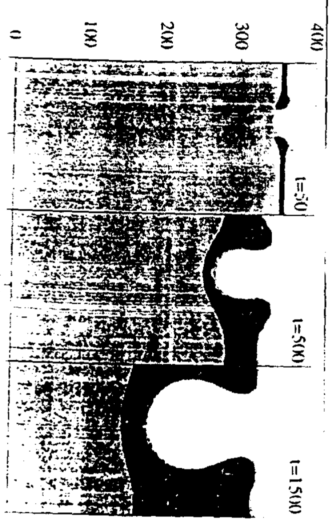

FIG. 1. The magnetic field B in the x-y plane, for a type-I superconductor in the *nucleation* regime, from Eqs. (4) and (6). The lengths are in units of the penetration depth $\lambda(T)$, time is in units of the order-parameter relaxation time τ_R, the magnetic field is in units of $\sqrt{2}H_c$, and the grey scale ranges from white ($B = 0$) to black ($B \approx H_c$). The external magnetic field is $H_e = 0.4$, $\kappa = 0.3$, and $\Sigma = 0.1$ (see text). We begin with a wedge-shaped perturbation on a planar superconducting-normal interface. The interface velocity is proportional to the field gradient, and the magnetic field is large in regions of negative curvature. These two features are expected on the basis of the simple diffusion model.

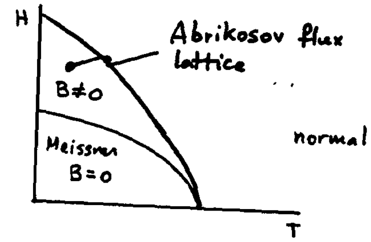

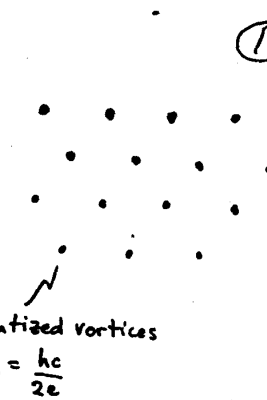

Negative surface tension in AFL phase. What happens to interface?

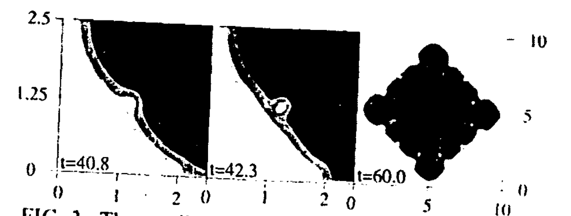

FIG. 3. The amplitude of the order parameter for a type-II superconductor. Here $\kappa = 20$, $H_e = 1.0$, and $\Sigma = 0.1$, and the grey scale ranges from white ($|\psi| = 0$) to black ($|\psi| = 1$); on the scale shown, the magnetic field varies very little from H_e. We start with a superconducting seed at the center of the lattice in a uniform magnetic field. It grows until vortex absorption becomes energetically favorable. The first two panels show the absorption of a single vortex at the interface: The vortex enters at a corner of the computational lattice. The third panel shows (i) the effect of the fourfold symmetry of the lattice on the large-scale shape of the superconducting region, and (ii) the stability [on lengths larger than $\lambda(T)$] of a planar interface.

19

Propagating Front Solutions in One Dimension

- Dimensionless TDGL equations in one dimension ($\psi = fe^{i\theta}$, $\mathbf{q} = \mathbf{A} - \nabla\theta/\kappa$):

$$\partial_t f = \frac{1}{\kappa^2}\partial_x^2 f - q^2 f + f - f^3,$$
$$\bar{\sigma}\partial_t q = \partial_x^2 q - f^2 q.$$

Both diffusive ($v \sim t^{-1/2}$) and propagating ($v =$ constant) solutions exist.

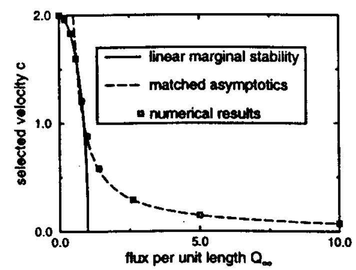

Figure 1: Numerical values (open squares) of the front speed as a function of Q_∞ for $\kappa = 1$ and $\bar{\sigma} = 1$.

- For propagating solutions, for small flux the problem reduces to *Fisher-KPP equation* (population biology); $v = 2/\kappa$. For large flux can use matched asymptotic expansions.
- For $\kappa = 1/\sqrt{2}$ and $\bar{\sigma} = 1/2$ the equations can be solved exactly,[6] with ($v = \sqrt{2}$).

[6] S. J. Di Bartolo and A. T. Dorsey, Phys. Rev. Lett. 77, 4442–4445 (1996).

20

Some experimental results

- M. R. Freeman, "Picosecond Studies of Nonequilibrium Flux Dynamics in a Superconductor," Phys. Rev. Lett. **69**, 1691 (1992).
- P. Leiderer *et al.*, "Nucleation and Growth of a Flux Instability in Superconducting $YBa_2Cu_3O_{7-x}$ Films," Phys. Rev. Lett. **71**, 2646 (1993).
- C. A. Duran *et al.*, "Observation of Magnetic Field Penetration via Dendritic Growth in Superconducting Niobium Films," Phys. Rev. B **52**, 75 (1995).
- H. D. Hallen *et al.*, "Penetration of Laterally Quantized Flux Lamina into a Superconducting Wire Network," Sol. State Comm. **99**, 651 (1996).
- Carina Reisin, "Flux Dynamics and Pattern Formation of Flux Penetration into Type-I Superconductors," doctoral thesis (Technion), 1997.

Demagnetizing effects and the intermediate state

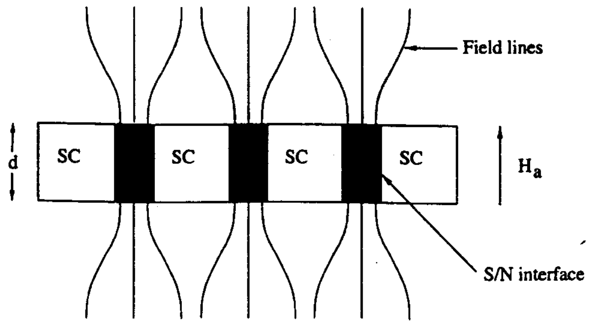

Side view

- In the film geometry the sample cannot expel the flux, so the superconducting and normal phases coexist.
- What sets the characteristic size of a domain? Need to account for
  - demagnetizing energy (bending of field lines), which favors a finely divided structure (energy $\sim a$);
  - surface energy of the interfaces, which favors a coarse structure (energy $\sim 1/a$).
- Minimizing, we find $a = \sqrt{\frac{d\Delta}{f(h)}}$, with d the film thickness, Δ the interfacial width (microscopic), and $f(h)$ a model dependent function of the reduced magnetic field $h = H_a/H_c$. Gives the correct order of magnitude.

Laminar Structure

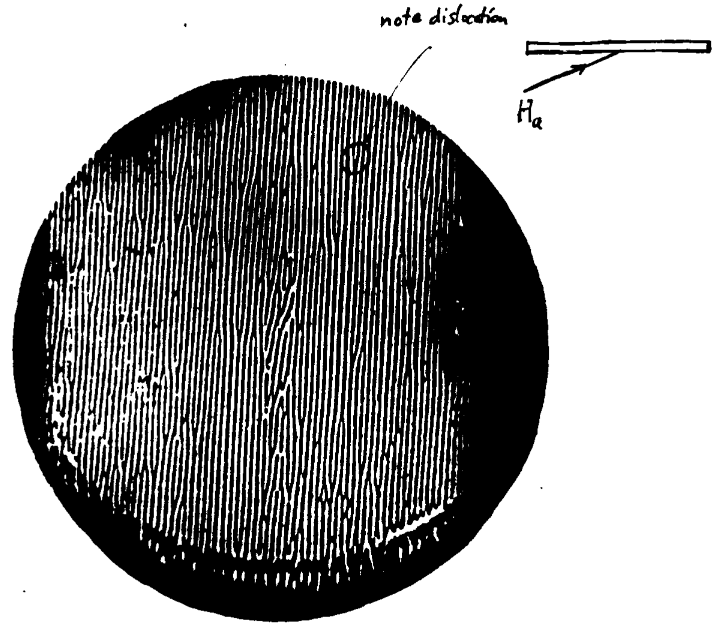

Fig. 8. Laminar structure observed in Sn disk in oblique field. $T = 2.165$°K, $h = 0.95$. Applied field makes an angle of 15° with the surface 1.8 X. In this photograph only, normal regions are dark. [After Sharvin (9).]

- Landau's structure is only observed in oblique fields.
- Laminar state the exception, not the rule.
- Other structures studied (Andrew 1948, Lasher 1967, Goren and Tinkham 1971, Callaway 1992). All regular.
- Need a more general approach for disordered patterns; dynamics.

23

Landau's theory of the intermediate state

- Assume a laminar structure:

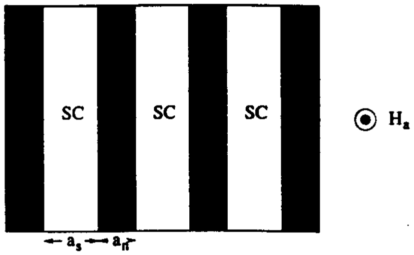

Top view

- The laminar structure is only observed experimentally in oblique fields.
- Global flux conservation: $H_a A = H_n A_n$, with $A = A_n + A_s$.
- Area fraction: $\rho_n = A_n/A = H_a/H_n$.
- Energy balance (bulk):

$$\mathcal{F} = \underbrace{-(H_c^2/8\pi)A_s d}_{\text{condensation energy}} + \underbrace{(H_n^2/8\pi)A_n d}_{\text{field energy}}.$$

- Minimum at $\rho_n = H_a/H_c$; i.e., $H_n = H_c$.
- Leaves out surface energy and demagnetizing effects. These require a model of the laminae shape.

24

Determining the shape of the laminae

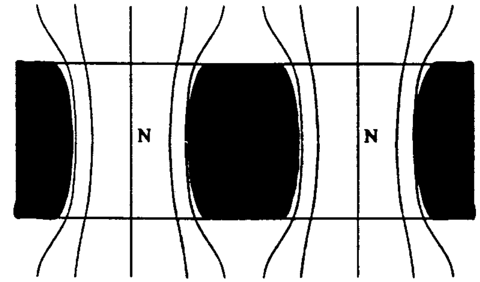

- Problem: find the shape of the laminae, determine the unknown $f(h)$.
- Two dimensional magnetostatics→ complex variable methods.
- Boundaries are unknown. Solve using the *hodograph method*; developed in the context of fluid mechanics:

Free streamline flow around a plate	**Laminae in superconductors**
Complex potential $w = \phi + i\psi$	**Complex potential $w = \phi + iA_y$**
Fluid velocity $u - iv = -dw/d\zeta$	Magnetic field $B = B_x - iB_z = -dw/d\zeta$
Streamlines	Field lines (lines of force)
Free streamline	Superconducting-normal interface
Free streamline velocity U	Superconducting critical field H_c
Region of fluid flow	Normal phase with nonzero magnetic field
Cavity behind plate	Superconducting phase
Riabouchinsky flow	Lamina in a finite thickness plate

The current loop (CL) model[7]

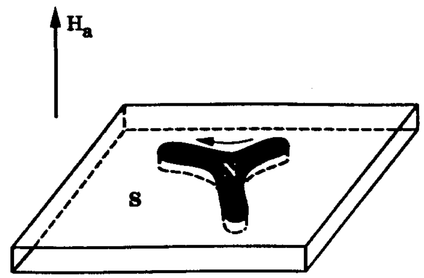

- What is the energy of a collection of normal domains of magnetization $M = -H_n/4\pi$?

$$E[\{\mathbf{r}_i\}] = \underbrace{V\frac{H_c^2}{8\pi}\rho_n}_{\text{condensation energy}} + \underbrace{V\frac{H_a H_n}{4\pi}(1-\rho_n)}_{\text{bulk field energy}}$$
$$+ \underbrace{\frac{H_c^2}{8\pi}\Delta d \sum_i L_i}_{\text{surface energy}} - \underbrace{\frac{1}{2}M^2 \sum_{i,j}\int_0^d dz \int_0^d dz' \oint ds \oint ds' \frac{\hat{\mathbf{t}}_i \cdot \hat{\mathbf{t}}_j}{R_{ij}}}_{\text{interaction among current loops}}.$$

- Assume the dynamics is overdamped:

$$\eta \partial_t \mathbf{r}_i(s) = -\frac{1}{\sqrt{g}}\frac{\delta E}{\delta \mathbf{r}_i(s)}.$$

- Can solve numerically using intrinsic coordinates (arclength and tangent angle).

[7] R. E. Goldstein, D. P. Jackson, and A. T. Dorsey, Phys. Rev. Lett. **76**, 3818–3821 (1996); A. T. Dorsey and R. E. Goldstein, Phys. Rev. B [redacted], 57, 3058 (1998)

Disordered patterns and instabilities

- Competition between long-range, repulsive interaction among the currents, and the surface tension, which is short range and attractive. For sufficiently small surface tension this results in a *branching instability*.
- Elongational instability of a circular flux domain, $h = 0.38$.

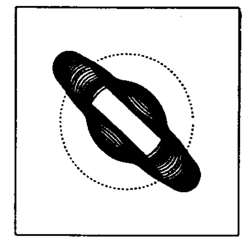

- Branching instability for $h = 0.45$.

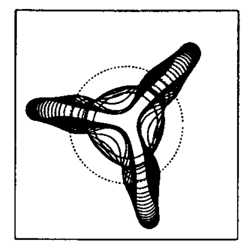

Energy of the laminar state in the CL model

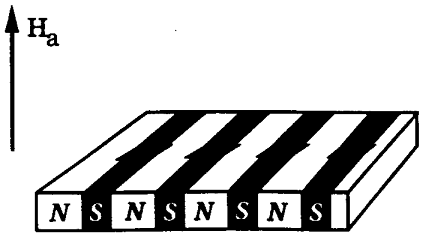

- The CL model captures many of the features of the disordered patterns. It can also be applied to the laminar state (observed in oblique fields).
- The function $f(h)$ calculated in the CL model is very close to $f(h)$ in the Landau model.
- Can use CL model to study the dynamics of the laminar state.
- Other periodic structures observed under some conditions: flux spots, honeycomb structures. Also, the thread model: E. R. Andrew, Proc. Roy. Soc. (London) **A194**, 98 (1948).

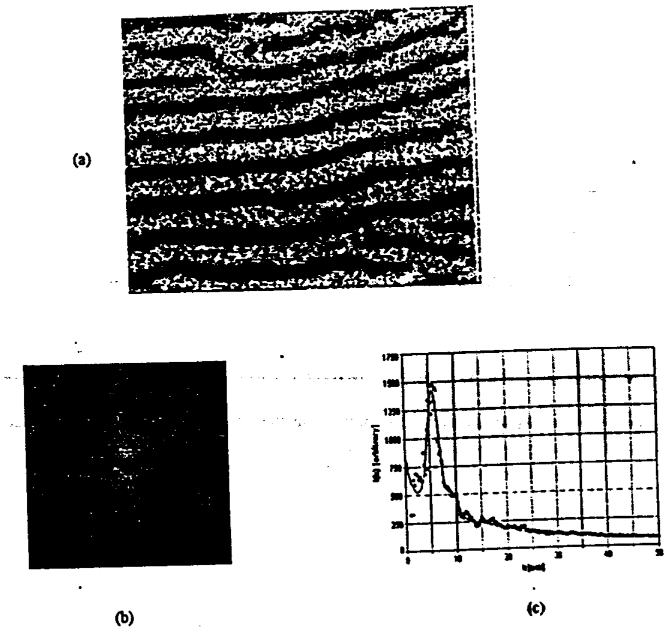

Figure 5.10 - Image analysis of laminar pattern: (a) typical laminar pattern (H=270 Gauss, β=20°). Normal regions are bright, superconducting regions are dark; (b) 2D fast-Fourier-transform of (a); (c) spectral intensity - experimental points (•), fitted curve (—).

איור 5.10 - ניתוח תמונה של תבנית למינרית: (a) תבנית למינרית טיפוסית, (H=270 Gauss, β=20°). אזורים נורמלים בהירים ואזורים מוליכי-על כהים, (b) התמרת פוריה 2D של (a). (c) עוצמה ספקטרלית - נקודות נסיוניות (•), עקומת התאמה (—).

C. Reisin, Ph.D. thesis (Technion)

C.R. Reisin and S. G. Lipson
Phys Rev B 61, 4251 (2000)

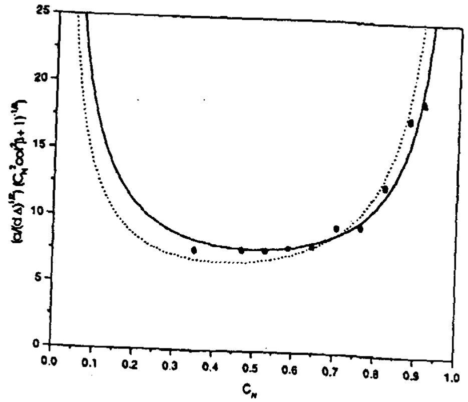

Fig. 4 Periodicity of laminar structures as a function of the reduced field, Landau nonbranching model (---) and GJD CL model (—) for Sharvin's geometry. The points are the experimentally observed periodicities scaled using Δ_L (○) and Δ_{CL} (•) [$(NI)_T$ transition].

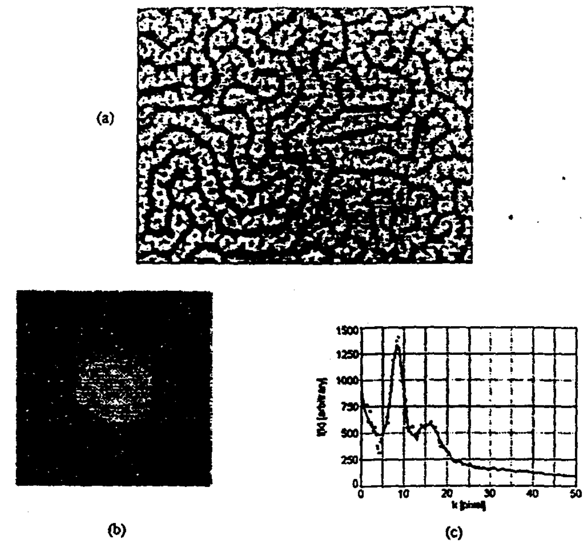

Figure 5.9 - Image analysis of corrugated pattern: (a) typical corrugated pattern, h=0.53. Normal regions are bright, superconducting regions are dark; (b) 2D fast-Fourier-transform of (a); (c) spectral intensity - experimental points (•), fitted curve (—).

איור 5.9 - ניתוח תמונה של תבנית מפותלת: (a) תבנית מפותלת טיפוסית, h=0.53. אזורים נורמלים בהירים ואזורים מוליכי-על כהים, (b) התמרת פוריה 2D של (a), (c) עוצמה ספקטרלית - נקודות נסיוניות (•), עקומת התאמה (—).

31

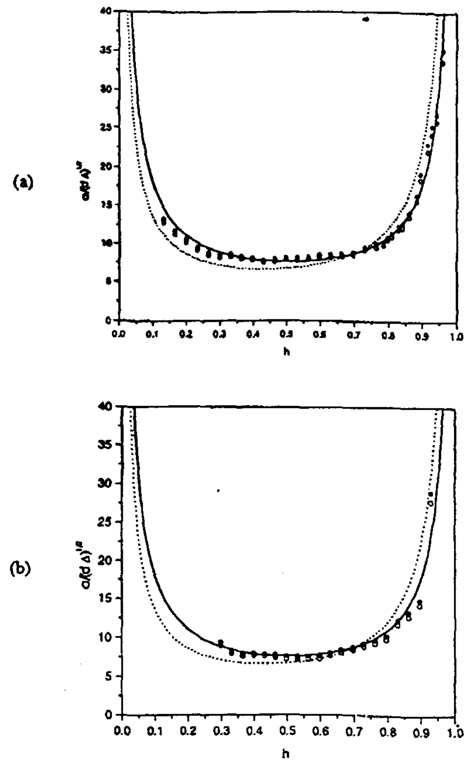

Fig. 2 Periodicity of corrugated structures as a function of the reduced field, Landau nonbranching model (---) and GJD CL model (—). The points are the experimentally observed periodicities scaled using Δ_L (∘) and Δ_{CL} (•): (a) $(NI)_T$ transition; (b) $(SI)_T$ transition.

206

32

Fluctuations and defects

- Can use CL model to examine deformations and fluctuations of the laminae.

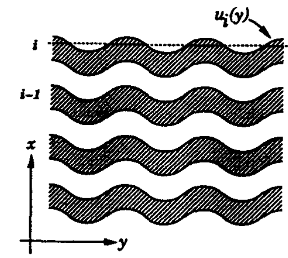

The *continuum elastic theory* is identical to that of a two-dimensional smectic liquid crystal:

$$\mathcal{F}_{\text{elastic}} = \int d^2r \left[\frac{B}{2} \left(u_x + \frac{1}{2} u_y^2 \right)^2 + \frac{K_1}{2} u_{yy}^2 \right].$$

- Can also include defects into the model in the form of *edge dislocations*; the dislocation energy is finite and can be small.

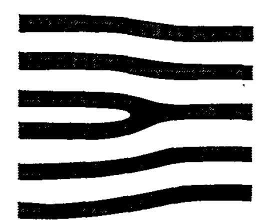

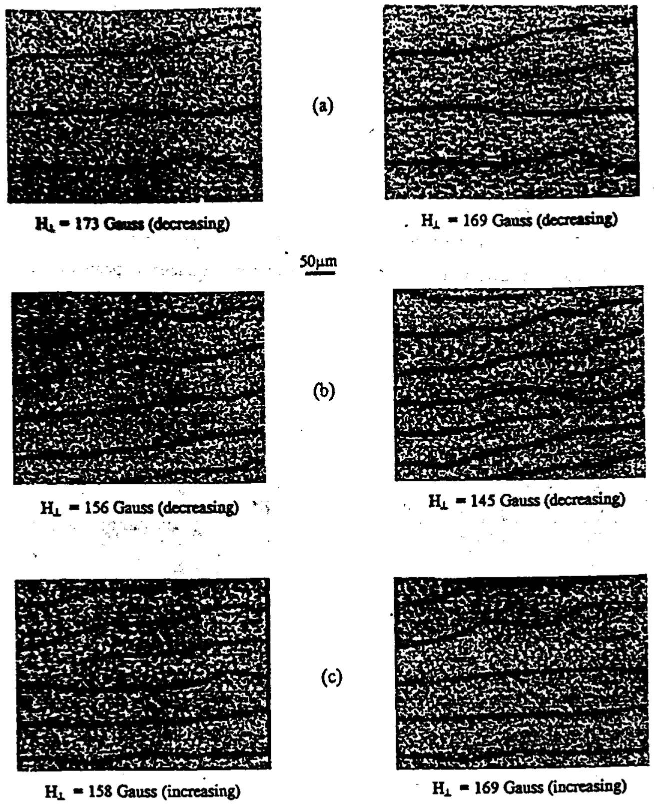

Figure 6.8 - Dislocation defects in laminar intermediate state pattern. Motion of laminae induced by changing the applied magnetic field: (a) and (b) climbing up, decreasing $H_\perp$, (c) climbing down, increasing $H_\perp$.

איור 6.8 - נקעים של פגמים בתבנית למינרית של מצב ביניים. תנועה למינה כתגובה לשינויים בשדה המגנטי המופעל: (a) ו- (b) טיפוס מעלה, הורדת $H_\perp$, (c) טיפוס מטה, העלאת $H_\perp$.

Some other labyrinthine patterns

- There are many other systems in which surface tension competes with long-range dipolar interactions; the energy is generally of the form

$$E[\{\mathbf{r}_i\}] = \Pi \sum_i A_i + \gamma \sum_i L_i - \frac{1}{2}\Omega \oint ds \oint ds' \hat{\mathbf{t}}_i \cdot \hat{\mathbf{t}}_j \Phi_{ij}(R_{ij}/\xi) .$$

System	Π	γ	Ω	Φ
type-I superconductors	$(H_c^2 d/8\pi)(\rho_n + h^2/\rho_n)$	$H_c^2 d\Delta/8\pi$	$H_n^2 d/8\pi$	$\sinh^{-1}(1/z)$ $+z-\sqrt{1+z^2}$
magnetic fluids	Lagrange multiplier	$d\sigma_{FW}$	$2dM^2$	$\sinh^{-1}(1/z)$ $+z-\sqrt{1+z^2}$
Langmuir monolayers	Lagrange multiplier	γ_{LE-LC}	$(\Delta\mu)^2$	$1/2z$
FitzHugh-Nagumo model	ΔF	$\bar{D}$	ρ	$K_0(z)$

Explanation of symbols: σ_{FW}, ferrofluid water surface tension; M, ferrofluid magnetization; γ_{LE-LC}, line tension between liquid expanded (LE) and liquid condensed (LC) phases in a Langmuir monolayer; $\Delta\mu$, discontinuity in electric dipole moment density between LE and LC phases; $d_{\rm mol}$, a molecular cutoff – monolayer thickness.

LABYRINTHS IN SUPERCONDUCTORS

• and magnetic fluids

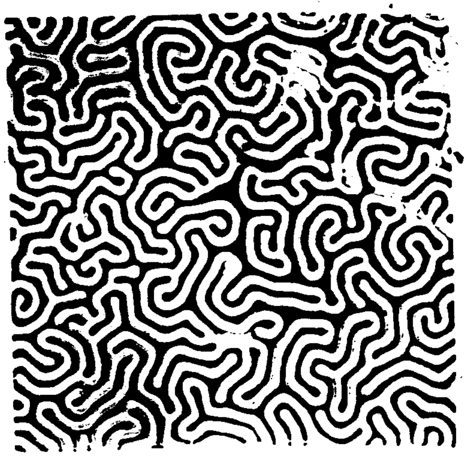

Summary

- Growth of the superconducting phase after a quench from the normal phase.
  - Growth limited by diffusion of magnetic flux away from the interface.
  - Interfacial instabilities lead to ramified patterns. Analogies with dendritic growth.
  - Behavior contained in simple free-boundary model is contained in TDGL equations.
- Structure of the intermediate state in type-I superconductors.
  - Introduced a current-loop model for the intermediate state.
  - For certain parameters the Biot-Savart interaction produces a branching instability.
  - CL model can also be applied to ordered structures such as the laminar state.
- Future work.
  - Phase ordering kinetics for layered systems. Dynamic scaling?
  - Go beyond relaxational dynamics and include diffusive dynamics. Easiest case—FitzHugh-Nagumo model (with R. Goldstein).
  - Pattern formation in type-II superconductors—flux invasion.

37

From Carlos Duran
AT&T Bell Labs   zfc   T=5.85 K
Nb film   Duran et al, Phys. Rev. B 52, 75 (1995).

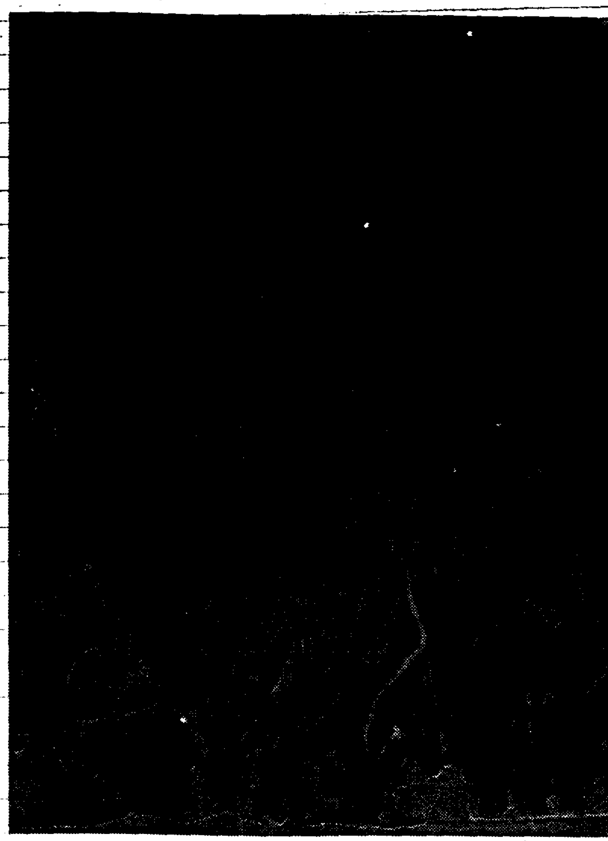

Normal phase (dark)
SC phase (light)